Supporting Material

Compartmentalized low-rank recovery for high resolution lipid unsuppressed MRSI

Ipshita Bhattacharya and Mathews Jacob

Dataset 1

	Mean	
	Lipid Rank=5	Lipid Rank = 20
NAA(2.008 ppm) attenuation (%)	$2.9X10^{-3}$ $2.80X10^{-3}$	$2.9X10^{-3}$ $2.81X10^{-3}$
Cre (3.027 ppm) attenuation (%)	$5.07X10^{-4}$ $4.74X10^{-4}$	$5.07X10^{-4}$ $4.76X10^{-4}$
Cho (3.185 ppm) attenuation (%)	$5.57X10^{-4}$ $5.15X10^{-4}$	$5.68X10^{-4}$ $5.21X10^{-4}$
Metabolite orthogonal energy projection to lipid subspace (%)	$1.19X10^{-3}$ $1.11X10^{-3}$	$1.2X10^{-3}$ $1.12X10^{-3}$
Lipid orthogonal energy projection to metabolite (Rank =15) subspace (%)	$1.63X10^{-4}$ $1.22X10^{-4}$	

Dataset 2

	Mean	
	Lipid Rank=5	Lipid Rank = 20
NAA(2.008 ppm) attenuation (%)	3.83 5.84	3.89 5.87
Cre (3.027 ppm) attenuation (%)	3.59 5.73	3.68 5.81
Cho (3.185 ppm) attenuation (%)	5.03 7.50	5.12 7.63
Metabolite orthogonal energy projection to lipid subspace (%)	3.182 6.582	3.183 6.583
Lipid orthogonal energy projection to metabolite (Rank =15) subspace (%)	3.155 6.516	

Dataset 3

	Mean	
	Lipid Rank=5	Lipid Rank = 20
NAA(2.008 ppm) attenuation (%)	4.72 6.78	4.90 7.01
Cre (3.027 ppm) attenuation (%)	5.01 7.14	5.07 7.21
Cho (3.185 ppm) attenuation (%)	5.98 8.36	6.09 8.49
Metabolite orthogonal energy projection to lipid subspace (%)	3.827 7.425	3.829 7.428
Lipid orthogonal energy projection to metabolite (Rank =15) subspace (%)	3.693 7.162	

Dataset 4

	Mean	
	Lipid Rank=5	Lipid Rank = 20
NAA(2.008 ppm) attenuation (%)	2.20 3.12	2.24 3.18
Cre (3.027 ppm) attenuation (%)	2.73 3.87	2.77 3.93
Cho (3.185 ppm) attenuation (%)	2.86 4.08	2.92 4.15
Metabolite orthogonal energy projection to lipid subspace (%)	1.673 3.298	1.674 3.299
Lipid orthogonal energy projection to metabolite (Rank =15) subspace (%)	1.649 3.251	

Metabolite attenuation and projection energies for metabolite lineshapes with FWHM = 10Hz , FWHM = 20 Hz

Figure S1: The tables record the average case(mean) percentage attenuation of metabolite intensities due to orthogonal projection and the orthogonal projection energy of the metabolites to the weighted lipid subspace (as shown in Fig. 4) for the four datasets. The orthogonal energy is small which supports our assumption. The effect of changing rank is studied with a rank=5 lipid subspace; the projection energy change due to rank is negligible. The mean orthogonal projection energy of lipid lineshapes on a weighted metabolite subspace of rank=15 is reported and is found to be very small.

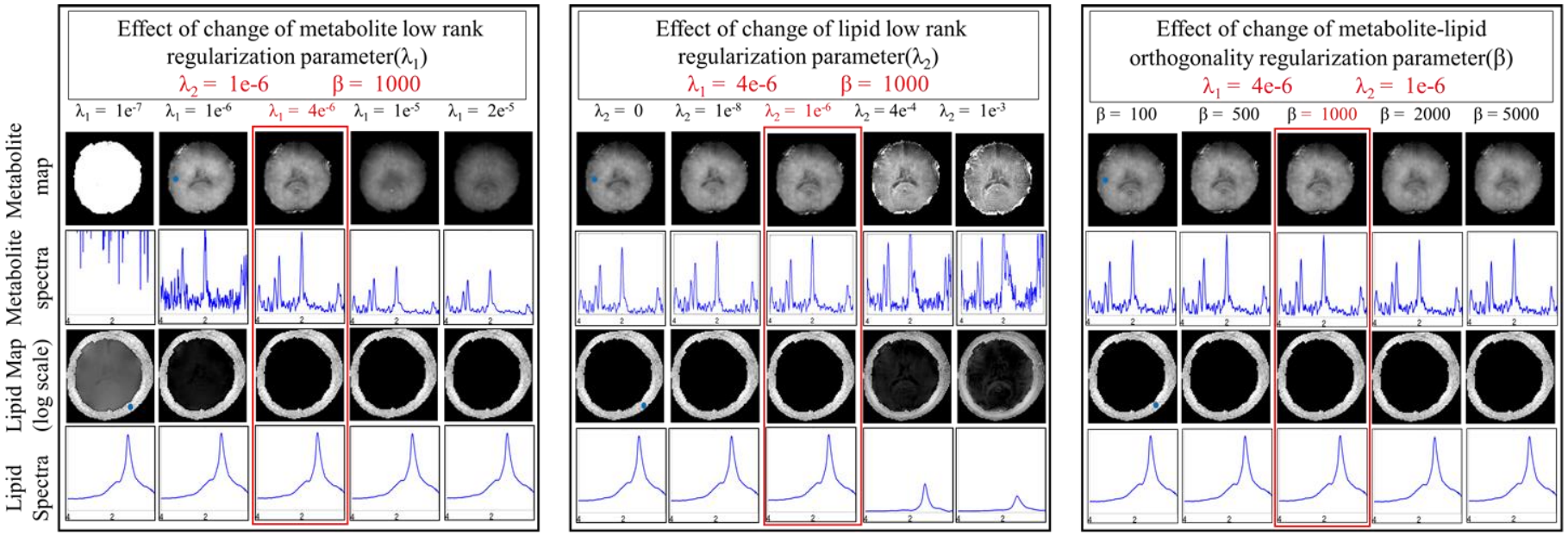

Figure S2: Effect of selecting different regularization parameter of the algorithm: The resulting reconstruction with varying regularization parameters are shown. The left block shows the effect of increasing λ_1 for fixed $\lambda_2 = 1e^{-6}$ & β = 1000. With increasing low-rank penalty on metabolites, the spectra (at the blue marked pixel in the second metabolite map) become more denoised and decreases in intensity whereas the spatial details are lost. We choose an intermediate value of $\lambda_1 = 4e^{-6}$ so as to achieve a balance between loss of spatial details and denoising spectra. There is no change in lipid maps or spectra (at the blue marked pixel in the first lipid map). In the middle block, effect of increasing λ_2 is shown for fixed $\lambda_1 = 4e^{-6}$ & β = 1000. As λ_2 increases lipid signal attenuates as seen from the maps and spectra. This also results in noisier metabolite spectra (at the blue marked pixel in the first metabolite map) and more spectral leakage at the edges. But choosing λ_2 as $1e^{-6}$ provides slight increase in metabolite peak heights, which is otherwise attenuated for a unregularized lipid compartment (as seen for λ_2 = 0 or $1e^{-8}$). The last block shows effect of changing β. For any high enough value, orthogonality constraint is imposed without discernible change in reconstruction performance. For very high values of β some spatial details are lost, most likely due to poor convergence.